P 1.4 MODEL SENSITIVITY STUDY AND STATISTICAL PRECIPITATION VALIDATION OF THE 11 JUNE 2000 NOCTURNAL MCS IN NEBRASKA

David B. Radell*, Clinton M. Rowe and Mark R. Anderson
Department of Geosciences, University of Nebraska-Lincoln, Lincoln, NE, USA

1. INTRODUCTION

In the data-sparse region of north-central Nebraska, convective precipitation forecasting and validation is a difficult task. Operational meteorologists must often rely on numerical output of quantitative precipitation forecasts (QPF) when forecasting in this region during the warm season. Improvement of QPF accuracy was labeled a priority by the National Center for Environmental Prediction (NCEP) as well as the general meteorological research community (Fritsch et al., 1998). Moreover, research has shown mesoscale convective systems (MCS) can be responsible for a significant portion of the Central Plains' yearly warm season precipitation total, adding to the importance of improving accurate prediction. Recently, however, many researchers (Colle and Mass, 2000; McBride and Ebert, 2000) have noted that much improvement is still needed for warm season events. The motivation for this experiment is the thorough testing and evaluation of model output over a relatively small domain to assess QPF performance over this geographically limited area.

An initial step to evaluate this issue was explored with a numerical simulation of an MCS that occurred over north-central Nebraska during the overnight hours of 11 June 2000. At its mature stage, the MCS contained both an intense convective leading edge accompanied by a large trailing stratiform region, providing an interesting challenge for a numerical model to effectively simulate. In this study, the PSU/NCAR MM5 was used to conduct a 48-hour simulation of the event with a triple-nested mesh and horizontal resolutions of 36, 12 and 4 km (Figure 1). Model generated precipitation patterns were examined under a variety of numerical experiments for the MCS. Statistical measures of model performance of precipitation such as bias, mean error, threat score, Kupiers' skill score and Heidke score were compiled and analyzed.

Overall, it is shown that the choice of cumulus parameterization scheme played the biggest role in dictating the resulting precipitation patterns, due mainly to the timing of convective initiation. Little increase in skill was noted between sensitivity studies of horizontal resolution, with precipitation amounts differing only by hundredths of an inch with negligible differences in spatial coverage.

**Corresponding author address*: David B. Radell, Meteorology/Climatology Program, 214 Bessey Hall, University of Nebraska-Lincoln, Lincoln, NE, 68508.
Email: dradell@papagayo.unl.edu

2. SYNOPTIC CONDITIONS

The upper air pattern prior to convection was typical for the time of year. Namely, the 250 hPa flow (not shown) was southwesterly at 45-50 kts over the Central Plains. Southwesterly flow continued at the 500 hPa level at approximately 25 kts. At 700 hPa, there was a trough evident in the ambient flow as a wind shift occurred from 0000 UTC 11 June to 1200 UTC 11 June. Winds were westerly at 20 kts and shifted to the south at 15-20 kts. This southerly flow increased dewpoints in the western High Plains by more than 15 °C. These southerly winds are also evident at 850 hPa.

Lower levels of the boundary layer recovered quickly from a cold front that moved through Nebraska on 10 June. The cold front transported moisture out of the region and did not produce any precipitation in Nebraska. The front stalled in the southeast corner of the state and dissipated slowly during the overnight hours of 11 June. The stalling of the front inhibited moisture return to the surface in the western parts of the state until after 0800 UTC. To the west, moisture-enhanced flow dominated until 1400 UTC. Southerly flow advected drier air into the southwestern portion of Nebraska. Moreover, southeasterly winds continued to transport moisture-laden air into north-central Nebraska. This enhanced moisture convergence in this region, particularly near Valentine (KVTN), NE. In the region with southerly winds (North Platte, NE, for instance), the dewpoints decreased over time. This resulted from the advection of relatively drier air found in northwestern Kansas compared to southeastern Nebraska. It is believed that this moisture discrepancy was the driving mechanism behind the convective development found in north-central Nebraska. This is in contrast to the lack of ambient moisture required for initiation to the south. Figure 2 displays the position of the surface features prior to initiation of the MCS.

3. MM5 CONFIGURATION AND METHODOLODY

Under a variety of model physics conditions, 48-hour simulations of the event were conducted using MM5 with a triple nest with the finest mesh centered over Broken Bow (KBBW), NE. The horizontal resolutions for domains 1,2 and 3 were 36 km, 12 km and 4 km, respectively with 139 x 208 grid points in domain 3. There are 23 levels in the vertical in terrain-following (?) coordinates. The model was initialized from the 40 km ETA 212 model as a first-guess. Routine surface and upper air National Weather Service (NWS) data were also used. The ETA 212 and NWS observations also served as boundary conditions every six hours during the model time integration. Each simulation was set up identically except for the choice of the model physics, where the cumulus parameterization, radiation scheme and microphysics were changed in a series of experiments. In choosing the physics options for the sensitivity studies, those referenced in the literature (see Wang, et al., 1997 for example) and used in other successful MM5 simulations of severe convective events were employed. Acronyms for each experiment are given by the following notation: *cumulus parameterization scheme; cloud microphysics; radiative transfer scheme*. For example, the GRGR run indicates that the Grell, Goddard, and RRTM options were used for that model run. Table 1 displays the matrix of sensitivity runs performed for this case. The MRF boundary layer option and OSU land surface model were also chosen for all three domains. Cumulus processes were resolved at the 36 and 12 km scales within the various cumulus parameterization schemes. At the 4 km resolution, no cumulus parameterization was used so that cumulus processes are explicitly resolved. To allow the model to "spin up" important physical processes such as vertical motions and cloud moisture, it was run 24-30 h prior to the occurrence of precipitation from the MCS.

Storm total precipitation patterns for each case were then analyzed and verified with WSR-88D estimated precipitation from the North Platte, NE radar (KLNX). Figure 3 shows the KLNX estimates from the MCS, with precipitation values exceeding 8 in. in northern Cherry County, near the South Dakota border. A secondary maximum exists just northwest of North Platte with values also nearing the 8 in. mark. According to storm reports and vertically integrated liquid (VIL) amounts, hail associated with the event did not exceed 2 in. and thus contamination of the radar estimated precipitation is unlikely. The estimated amounts were then interpolated to a grid identical in size to the MM5 domain 3 (136 x 208 points), where "nearest neighbor" grid point precipitation values were assigned to the new grid. To verify statistically precipitation amounts with MM5 output, results from regions containing the majority of the spatial coverage and maximum intensities were employed. Two methods of data comparison were used in this study. First, precipitation was analyzed in a subsection of the model domain, as shown in Figure 3, outlined in white. These 1°x 2° boxes (labeled zones 1 and 2) were chosen to coincide both with the approximate path of the propagating MCS as well as the regions of maximum observed precipitation. Within this region, point-by-point comparisons as well as zone averaged and maximum precipitation values were analyzed. The zonal averages and maximums amounts of precipitation were calculated to account for the spatial variations which were observed in several of the runs.

4. DISCUSSION

Figure 4 displays the calculated bias and threat scores on a point-by-point comparison for zones 1 and 2 for a 0.1 in. threshold. It is apparent that both the BM and KF runs underestimated the overall precipitation, often by 25% or more. The GR runs seemed to better capture the actual precipitation, though overestimating the amounts by approximately 10%. It is interesting to note that the threat scores, defined as the number of hits less the correct "no" forecasts, do not significantly vary between any of the runs. Thus, for the GR runs the improved bias scores over the others are due to the better estimates of spatial coverage within the zones, not correctly forecasting amounts at more grid points. This is evident in the model precipitation fields (not shown) with the GR runs producing spatially more precipitation in both zones.

From the same figure, another pattern is seen between radiation schemes within the Goddard and Reisner microphysics. There is an improvement from the CCM2 to RRTM within the Resiner scheme while a decrease exists within the Goddard runs. One possibility for these differences is the amount of cloud water predicted by each microphysics scheme. Preliminary analysis shows that the Reisner scheme runs generally predicted more cloud water than its Goddard counterpart. Thus, as this was a nocturnal event, the RRTM handled the longwave radiation interactions with clouds better than the CCM2, and less so without cloud matter. This hypothesis needs to be further investigated, and is beyond the scope of this paper to provide additional detail. Overall, the values of the bias and threat scores match or are slightly greater than those noted in other modeled warm season studies (see Wang and Seaman 1997; McBride and Ebert 2000, for example).

Figure 5 displays the mean error at all grid points for both zones. As expected, the underforecasted model runs exhibit negative mean errors, indicative of both the lack of coverage and intensity which were more accurately predicted in the GR runs. Figure 6 displays the Kupiers' and Heidke skill scores for point-by-point (0.1 in. threshold) comparisons within zones 1 and 2. These measures of predictive skill vary between ±1, with +1 indicating a perfect forecast, 0 a random forecast and –1 referring to a forecast inferior to a random forecast. These results indicate that the BM runs exhibited the best skill, while GR and KF were overall only slightly better than a random forecast. The Resiner scheme seems to produce the best skill within each cumulus parameterization scheme. The large negative value seen in the GRGR run indicates an extraordinarily large number of "yes" forecasted and "no" observed or "no" forecasted and "yes" observed values within the zones, and is evident in a plot of isoheyts (not shown) with only 2 spurious maximum within the zones.

To account for spatial discrepancies within successive model runs, zonal averages were calculated and compared. Maximum precipitation values were also determined. Figure 7 shows a plot of the observed and modeled maximum precipitation for both zones as well as the time of convective initiation for each run. A relationship is noted between maximum predicted amount of precipitation and time of initiation. Within the GR runs, the MCS initiated a few hours earlier compared to the other runs and subsequently captured peak rainfall amounts for each zone more accurately. Thus, the initiation trigger functions within each cumulus scheme play a major role in determining peak rainfall amounts within each zone. Further analysis into the specific triggering mechanisms needs to be undertaken for better analysis. For example, as convective available potential energy values (CAPE) at a grid point in the KF scheme determine convection, comparative plots between all runs would more accurately assess the onset of precipitation. Further, the BM runs lack a parameterized downdraft, which is present in the other schemes, and may lead to an overall lack of modeled structure of the MCS and in turn produces less overall precipitation. Preliminary investigations show that the GR and KF runs capture the large outflow seen in radar observations produced by the MCS. No such feature exists within the BM runs.

This study was designed to gain further insight into the differences in varying the model physics for a warm season convective event. Initial conclusions indicate that the Grell scheme combined with Reisner microphysics overall better predicted the position, spatial coverage and intensity of precipitation for this event. Additional research is needed to assess the role of cloud cover and radiation effects as well as the convective trigger function in each case for further results.

5. ACKNOWLEDGEMENTS

This project was partially supported by the NOAA/NASA GAPP Program. We also thank the Research Computing Facility at the University of Nebraska for use of their supercomputers.

6. REFERENCES

Colle, B.A., and C.F. Mass, 2000: The 5-9 February 1996 flooding event over the Pacific Northwest: Sensitivity studies and evaluation of the MM5 precipitation forecasts. *Mon. Wea. Rev.*, **128**, pp. 593-617.

Fritsch, J.M. and Coauthors, 1998: Quantitative precipitation forecasting: Report of the eighth prospectus development team, U.S. Weather Research Program. *Bull. Amer. Meteor. Soc.*, **79**, pp. 285-299.

McBride, J.L., and E.E. Ebert, 2000: Verification of quantitative precipitation forecasts from operational numerical weather prediction models over Australia. *Wea. Forecasting*, **103**, pp. 103–121.

Wang, W., and N. L. Seaman, 1997: A Comparison Study of Convective Parameterization Schemes in a Mesoscale Model. *Mon. Wea. Rev.*,**125**, pp. 252–278.

7. FIGURES

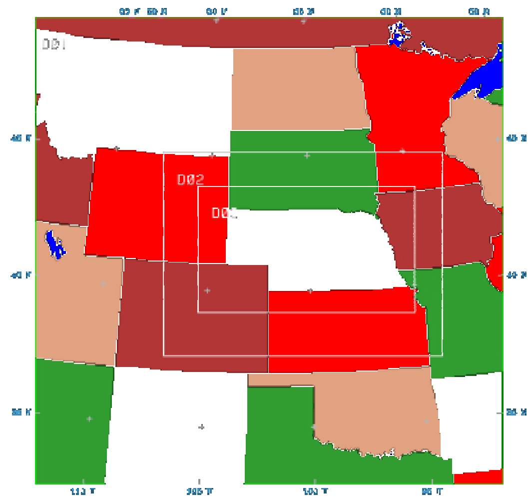

FIGURE 1. MM5 domains used in this study.

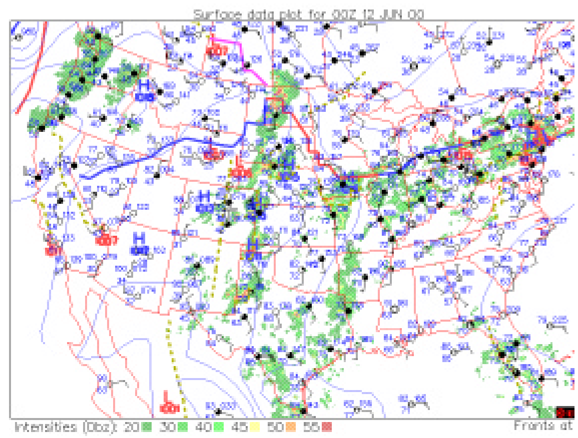

Figure 2. Surface conditions valid 0000 UTC 12 June 2000.

MICRO-PHYSICS	Goddard	Schultz	Reisner
ICUPA			
Kain-Fritsch	KFGR KFGC	KFSR KFSC	KFRR KFRC
Grell	GRGR GRGC	GRSR GRSC	GRRR GRRC
Betts-Miller	BMGR BMGC	BMSR BMSC	BMRR BMRC

TABLE 1. Matrix of MM5 sensitivity studies.

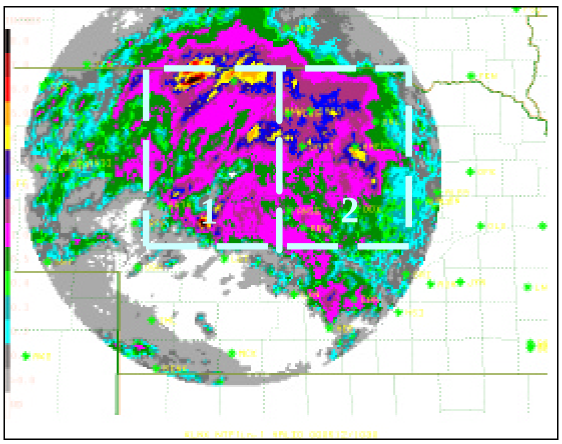

FIGURE 3. WSR-88D image of storm total precipitation (in.) from North Platte, NE (KLNX).

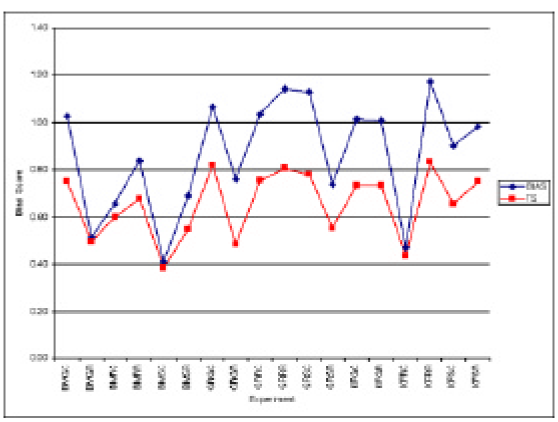

FIGURE 4. Bias score (BS) and threat score(TS) for each experiment.

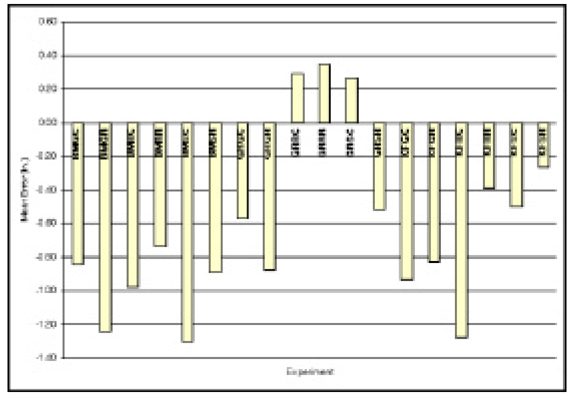

FIGURE 5. Mean error (ME, in.) for each experiment.

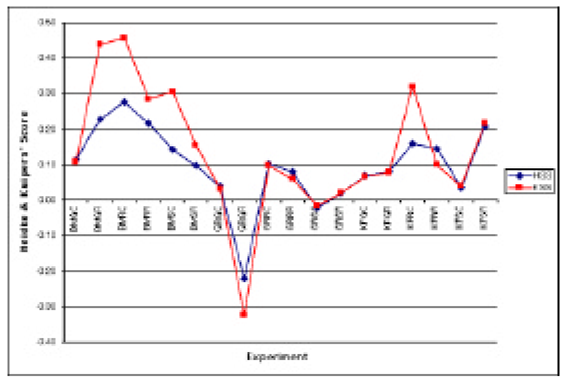

FIGURE 6. Heidke and Kupiers' skill scores for each experiment.

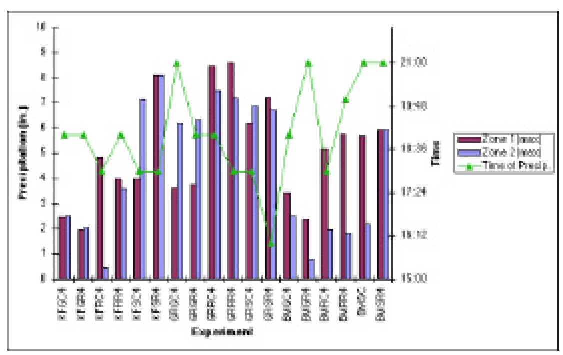

FIGURE 7. Time of model convective initiation and maximum zonal precipitation.